European Journal of Medicinal Chemistry 46 (2011) 5790–5799

Contents lists available at SciVerse ScienceDirect

European Journal of Medicinal Chemistry

journal homepage: http://www.elsevier.com/locate/ejmech

Original article

New spirocyclic Δ^2-isoxazoline derivatives related to selective agonists of α7 neuronal nicotinic acetylcholine receptors

Clelia Dallanoce[a,*], Fabio Frigerio[a], Giovanni Grazioso[a], Carlo Matera[a], Giacomo Luca Visconti[a], Marco De Amici[a], Luca Pucci[b], Francesco Pistillo[c], Sergio Fucile[c,d], Cecilia Gotti[b], Francesco Clementi[b], Carlo De Micheli[a]

[a] Dipartimento di Scienze Farmaceutiche "Pietro Pratesi", Università degli Studi di Milano, Via Mangiagalli 25, 20133 Milano, Italy
[b] CNR, Istituto di Neuroscienze, Farmacologia Cellulare e Molecolare e Dipartimento di Farmacologia, Chemioterapia e Tossicologia Medica, Università degli Studi di Milano, Via Vanvitelli 32, 20129 Milano, Italy
[c] I.R.C.C.S. Neuromed, Istituto Neurologico Mediterraneo, Via Atinese 18, 86077 Pozzilli (Isernia), Italy
[d] Dipartimento di Fisiologia e Farmacologia, Università di Roma La Sapienza, Piazzale A. Moro 5, 00185 Roma, Italy

ARTICLE INFO

Article history:
Received 28 February 2011
Received in revised form
12 July 2011
Accepted 19 September 2011
Available online 24 September 2011

Keywords:
Neuronal nicotinic acetylcholine receptors
α7 Selective nicotinic ligands
Cycloaddition reaction
Binding affinity
Electrophysiological assays
Molecular modeling

ABSTRACT

A set of structural analogues of spirocyclic quinuclidinyl-Δ^2-isoxazolines, characterized as potent and selective α7 nicotinic agonists, was prepared and assayed for binding affinity at α7 and α4β2 neuronal nicotinic acetylcholine receptors (nAChRs). The investigated derivatives (**3a**–**3c**, **4a**–**4c**, **5a**–**5c**, **6a**–**6c**, and **7a**–**7c**), synthesized via the 1,3-dipolar cycloaddition of nitrile oxides to suitable dipolarophiles, showed an overall reduced affinity at the α7 subtype when compared with their model compounds. Solely Δ^2-isoxazolines **3a**, **3b**, and **6c** maintained a binding affinity in the nanomolar range at the α7 nAChRs (K_i = 230, 420 and 700 nM, respectively). The quaternary ammonium salt **6c** retained also a noteworthy α7 vs. α4β2 subtype selectivity, whereas **3a** and **3b** showed a sharp reduction in selectivity compared with **1a** and **1b**, their quinuclidinyl higher homologues.

1. Introduction

Nicotinic acetylcholine receptors (nAChRs) are broadly characterized transmembrane proteins which mediate the physiological responses to the neurotransmitter acetylcholine. These receptors, which are expressed in muscle, nerve and sensory cells, exist as pentameric ligand-gated ion channels composed of α (α1-α10) and non-α (β1-β4, ε, γ, and δ) subunits [1,2]. Homomeric channels are composed of α7 or α9 subunits and the α10 subunit only gives rise to functional receptors when it is co-expressed with the α9 subunit. Among the subunits which form homomeric nAChRs, only the α7 one is widely distributed in the mammalian brain. The α2-α6 and β2-β4 subunits generate an array of heteromeric channels found in the central nervous system (CNS), and much effort is currently devoted to completing the knowledge of their structure, distribution, and physiological role [3,4]. The heteromeric α4β2 and the homomeric α7 subtypes have been characterized as the most prominent nAChRs in the CNS, especially in brain areas (cortex and hippocampus) involved in the elaboration of cognitive processes [3]. These two receptor subtypes also modulate the release of neurotransmitters such as acetylcholine, glutamate, γ-aminobutyric acid, norepinephrine, histamine and dopamine, which are essential for a wide range of CNS functions [3,5]. Functionally, α7 channels are distinguished from α4β2 receptors due to their lower affinity for acetylcholine, high affinity for the antagonist α-bungarotoxin, fast desensitization, and higher permeability to calcium [3,4,6]. In the last two decades, an improved knowledge of the role exerted by the two cited nAChR subtypes in cognitive processes, mood, nociception, and neuroprotection has engendered the development of subtype-selective compounds with therapeutic potential for different CNS-related pathologies, including Alzheimer's and Parkinson's diseases, attention deficit hyperactivity disorder, schizophrenia, epilepsy, Tourette's syndrome, anxiety, depression, and nicotine addiction [4,7]. Moreover, homopentameric α7 channels were found to exert a pivotal role in mediating most of the anti-inflammatory effect of the vagal cholinergic pathway [8]. Consequently, selective α7 agonists have been

* Corresponding author. Tel.: +39 02 50319327; fax: + 39 02 50319326.
E-mail address: clelia.dallanoce@unimi.it (C. Dallanoce).

0223-5234/$ – see front matter © 2011 Elsevier Masson SAS. All rights reserved.
doi:10.1016/j.ejmech.2011.09.028

investigated in different experimental models of inflammation, thus providing additional insight into the functional biology of this nAChR subtype [8]. Furthermore, an anti-neuropathic effect has been recently demonstrated, in terms of pain behavior and nervous tissue protection, following acute and repeated treatment with α7 selective agonists in a model of peripheral neuropathy [9].

The structural requirements of ligands selectively binding to α7 or α4β2 nAChR subtypes have been the subject of a number of investigations, whose most relevant results were collected in comprehensive literature reports [4,7a]. Interestingly, in a recent study, novel molecular scaffolds were identified, capable to generate high selectivity at α7 or α4β2 nAChR subtype with simple changes in the substitution pattern [10]. These structural variations on a common molecular skeleton should contribute to better define differences in the ligand binding domains of the two investigated nAChRs, particularly in receptor areas outside the conserved cation binding crevice [10].

In the last years, our research group has been involved in the study of the structure–activity relationships of a number of heterocyclic derivatives designed as selective ligands for neuronal nAChR subtypes [11]. In this framework, we patented a series of compounds targeting the α7 subtype [12a], and, among them, the spirocyclic quinuclidinyl-Δ^2-isoxazolines **1a**–**1c**, **2a** and **2b** (Fig. 1) emerged as the most selective α7 vs. α4β2 ligands [12b]. In this paper, we discuss the preparation and pharmacological characterization of a group of structural analogues of the above cited quinuclidinyl derivatives, i.e. their lower homologues containing the 1-azabicyclo[2.2.1]heptane nucleus as well as simplified analogues carrying the piperidine or the *N*-methylpiperidine moiety. Herein we report the synthesis and the binding affinity data at α7, α4β2 and α3β4 nAChRs of spirocyclic derivatives **3a**–**c**, **4a**–**c**, **5a**–**c**, **6a**–**c**, and **7a**–**c** (Fig. 1). We chose to investigate even the quaternary ammonium salts **4a**–**c** and **6a**–**c** in view of a potential interest in selective ligands targeting the peripheral α7 nAChR population.

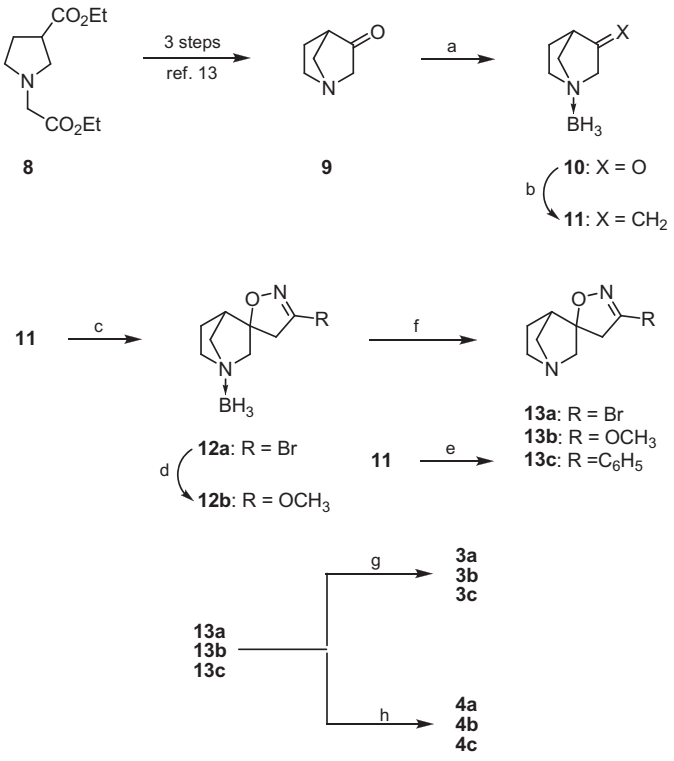

Scheme 1. Reagents and conditions: (a) 1.0 M BH_3-THF complex (1 equiv), THF, r.t., 10 min; (b) $CH_3P(C_6H_5)_3Br$ (1.5 equiv), *tert*-BuOK (1.4 equiv), THF, reflux 45 min, then r.t., 1h; (c) Br_2C = NOH (1.1 equiv), $NaHCO_3$, AcOEt, r.t., 48 h; (d) K_2CO_3, MeOH, reflux, 4 h; (e) PhCH = NOH (2.5 equiv), 3.5% aq NaClO (2.5 equiv), CH_2Cl_2, r.t., 13 h; (f) CF_3CO_2H (7 equiv), acetone, r.t., 10 h; (g) $C_4H_4O_4$ (1.1 equiv), MeOH, r.t., 16 h; (h) CH_3I (10 equiv), Et_2O, r.t., 1 h.

2. Chemistry

All spirocylic derivatives were synthesized as racemates taking advantage of the 1,3-dipolar cycloaddition of nitrile oxides to properly protected dipolarophiles [11c,12]. As illustrated in Scheme 1, diester **8** was initially converted into 3-oxo-1-azabicyclo[2.2.1]heptane **9** following an experimental protocol described in the literature [13]. Treatment of **9** with a 1.0 M solution of borane-THF complex provided the *N*-boranyl ketone **10**, which underwent a smooth Wittig-type methylenation to afford alkene **11**. The latter was used as the dipolarophile in the pericyclic reactions with bromonitrile oxide and benzonitrile oxide. In both cases, the 1,3-dipole was generated in situ from a stable precursor, i.e. dibromoformoxime [14a] or benzaldoxime [14b].

1a: R = Br
1b: R = OCH_3
1c: R = C_6H_5

2a: R = Br
2b: R = OCH_3

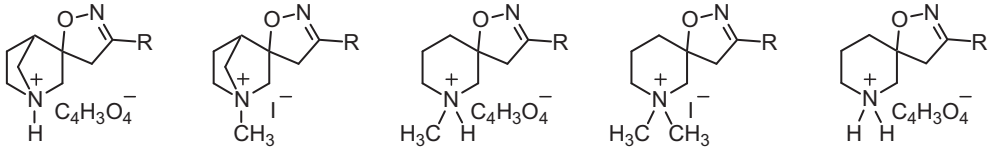

3a: R = Br
3b: R = OCH_3
3c: R = C_6H_5

4a: R = Br
4b: R = OCH_3
4c: R = C_6H_5

5a: R = Br
5b: R = OCH_3
5c: R = C_6H_5

6a: R = Br
6b: R = OCH_3
6c: R = C_6H_5

7a: R = Br
7b: R = OCH_3
7c: R = C_6H_5

Fig. 1. Molecular structure of model and target compounds.

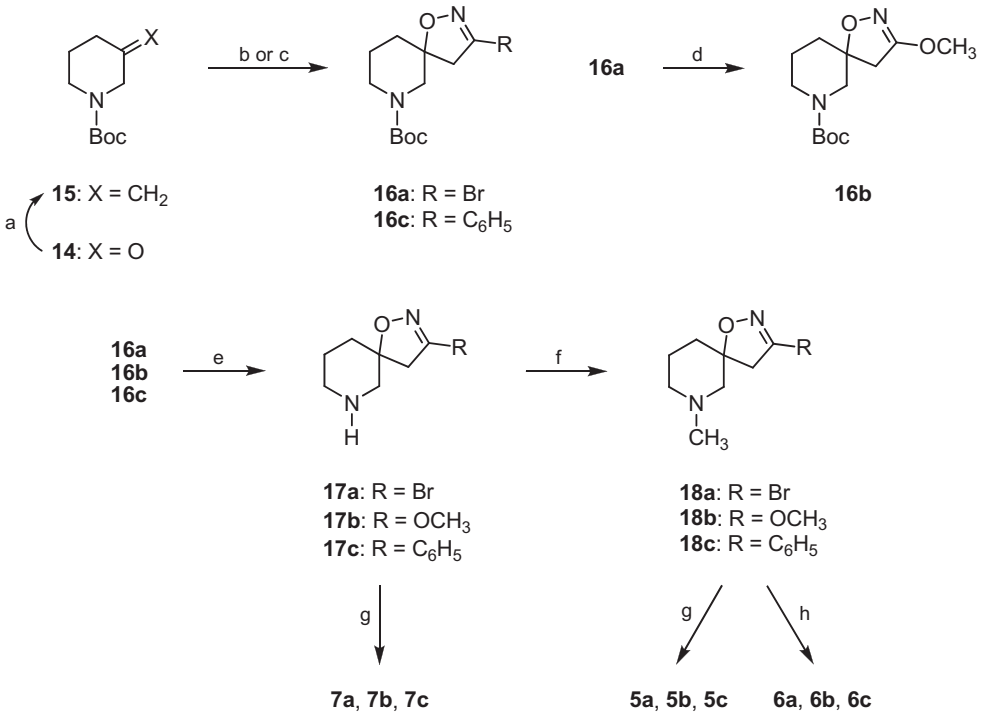

Scheme 2. Reagents and conditions: (a) $CH_3P(C_6H_5)_3Br$ (1.5 equiv), *tert*-BuOK (1.4 equiv), THF, reflux 45 min, then r.t., 1 h; (b) $Br_2C=NOH$ (1.1 equiv), $NaHCO_3$, AcOEt, r.t., 48 h; (c) PhCH = NOH (2.5 equiv), 3.5% aq NaClO (2.5 equiv), CH_2Cl_2, r.t., 13 h; (d) K_2CO_3, MeOH, reflux, 4 h; (e) 4N HCl (1.6 equiv), dioxane, r.t., 1 h (for **17a**) or CF_3CO_2H (7 equiv), CH_2Cl_2, r.t., 10 h (for **17b** and **17c**); (f) 37% aq HCHO (5 equiv), $NaBH_3CN$ (2.5 equiv), CH_3CN, r.t., 20 min; (g) $C_4H_4O_4$ (1.1 equiv), MeOH, r.t., 16 h; (h) CH_3I (10 equiv), Et_2O, r.t., 1 h.

Worth noting, while the first cycloaddition gave the expected 3-bromo-*N*-boranyl derivative **12a** in 88% yield, the second one did not produce the corresponding 3-phenyl analogue but directly the *N*-deprotected derivative **13c** in less than 10% yield. The 3-bromo intermediate **12a** was submitted to the nucleophilic displacement by methanol to provide the corresponding 3-methoxy derivative **12b** in high yield. The *N*-boranyl group of compounds **12a** and **12b** was then removed by treatment with a dichloromethane solution of trifluoroacetic acid to yield the desired tertiary bases **13a** and **13b**, respectively. Amines **13a**–**c** were then treated with fumaric acid to afford the related crystalline fumarates **3a**–**3c** or, alternatively, were transformed into the corresponding iodomethylates **4a**–**4c** by reaction with excess iodomethane (Scheme 1).

The *N*-Boc-3-methylenepiperidine **15**, obtained from commercially available *N*-Boc-3-piperidone **14** through a Wittig reaction, was submitted to the previously described cycloaddition reactions, as reported in Scheme 2. In this instance, both bromo- and phenyl-Δ^2-isoxazolines **16a** and **16c** were isolated in very high yield. Likewise, the transformation of the 3-bromo derivative **16a** into the corresponding 3-methoxy analogue **16b** occurred smoothly.

Table 1
Affinity of derivatives **3a**–**7a**, **3b**–**7b**, and **3c**–**7c** for native α7 and α4β2 nAChR subtypes present in rat cortical membranes, labeled by [^{125}I]α-bungarotoxin and [^{3}H] epibatidine. Affinity of derivatives **3a**–**3c**, **5b**, **6c**, **7b**, and **7c** for α3β4 nAChRs heterologously expressed in HEK 293 cells.

Compound	α7 [^{125}I]α–BgTx K_i[a] (μM), $n = 4$	α4β2 [^{3}H]Epibatidine K_i[a] (μM), $n = 4$	α3β4 [^{3}H]Epibatidine K_i[a] (μM), $n = 4$
1a × 0.5 $C_4H_4O_4$	0.0135 (29)[b]	0.64 (17)[b]	
1b × 1.5 $C_4H_4O_4$	0.0142 (32)[b]	7.90 (16)[b]	
1c × 0.5 $C_4H_4O_4$	0.025 (35)[b]	22 (21)[b]	
2a	0.109 (23)[b]	32.5 (18)[b]	
2b	0.0914 (36)[b]	175.4 (17)[b]	
3a × 0.75 $C_4H_4O_4$	0.23 (30)	5 (14)	13 (17)
3b × 0.5 $C_4H_4O_4$	0.42 (35)	16 (22)	46 (21)
3c × 0.5 $C_4H_4O_4$	3.60 (31)	53 (32)	16 (16)
4a	6.20 (46)	22 (20)	Nt
4b	2.90 (38)	20 (28)	Nt
4c	5.10 (48)	38 (31)	Nt
5a × 0.75 $C_4H_4O_4$	6.60 (53)	44 (38)	Nt
5b × 0.75 $C_4H_4O_4$	5.50 (42)	> 100	91 (18)
5c × 0.75 $C_4H_4O_4$	30 (44)	> 100	Nt
6a	3.70 (48)	50 (33)	Nt
6b	13 (48)	94 (32)	Nt
6c	0.70 (39)	> 100	6.60 (16)
7a × 0.5 $C_4H_4O_4$	4.30 (34)	58 (41)	Nt
7b × 0.5 $C_4H_4O_4$	3.70 (41)	> 100	75 (16)
7c × 0.75 $C_4H_4O_4$	4.50 (37)	> 100	43 (15)

[a] The K_i values were derived from three competition-binding experiments. The numbers in brackets refer to the % coefficients of variation.
[b] Ref. [12b]. Nt: not tested.

Removal of the *N*-Boc protective group from **16a**–**16c** was carried out under standard conditions to give secondary amines **17a**–**17c** in high yield (Scheme 2). The free bases were converted into the related fumarates **7a**–**7c** or were submitted to reductive amination with aqueous formaldehyde and sodium cyanoborohydride, to provide the corresponding tertiary amines **18a**–**18c** in 90–97% yield. The desired final salts were then obtained by treating these tertiary bases either with fumaric acid to give fumarates **5a**–**5c** or with methyl iodide to produce iodomethylates **6a**–**6c**.

3. Pharmacology

Target compounds **3a**–**7a**, **3b**–**7b**, and **3c**–**7c** were tested for binding affinity at rat α7 and α4β2 nAChR subtypes, using [^{125}I] α-bungarotoxin and [^{3}H]epibatidine as radioligands, respectively, according to a previously described experimental protocol [11c]. The K_i values, which were calculated from the competition curves of four separate experiments by means of the LIGAND program [15], are gathered in Table 1 and compared with those of reference analogues **1a**–**1c**, **2a**, and **2b** [12b]. We also evaluated the binding affinity of some of the derivatives under study, i.e. **3a**–**3c**, **5b**, **6c**, **7b** and **7c**, for heterologously expressed α3β4 nAChRs (Table 1). This subtype is predominant in sensory and autonomic ganglia and in the adrenal gland but it is also expressed in specific brain regions, where it seems to be involved in addiction to nicotine and other drugs of abuse [16a]. A relevant affinity for this "ganglionic nAChR subtype" [16b] could potentially cause relevant adverse effects in compounds designed as selective agonists at the α7 subtype.

The overall pharmacological data on the novel derivatives confirm that the quinuclidine moiety is a crucial structural requirement for the ligand recognition by the α7 nAChRs [17]. Indeed, derivatives **3a**–**3c**, which carry the 1-azabicyclo[2.2.1] heptane nucleus and are the closest analogues of template agonists **1a**–**1c**, show a significantly lower affinity than the reference compounds. As a matter of fact, the binding affinity of compounds **3a**–**3c** at the α7 subtype is 17-, 30- and 144-fold lower than that of the corresponding one carbon higher homologues **1a**–**1c**. Such a reduction can reasonably be ascribed to a shape modification of the basic portion of the ligands. Nevertheless, among the novel derivatives, the 3-Br (**3a**) and the 3-OCH_3 (**3b**) compounds displayed the highest affinity at α7 nAChRs (K_i values of 0.23 μM and 0.42 μM, respectively), thus paralleling the biological trend of leading compounds **1a** and **1b**.

The Δ^2-isoxazolines bearing either the piperidine (**7a**–**7c**) or the 1-methylpiperidine nucleus (**5a**–**5c**) behaved as low affinity α7 nicotinic ligands, with K_i values in the range 3.70–30 μM. Furthermore, they exhibited one order of magnitude lower affinity at the α4β2 subtype (K_i in the range 44 - > 100 μM) compared with that determined at the α7 subtype. Even the permanently charged methiodides **4a**–**4c**, **6a**, and **6b** can be classified as low affinity and unselective nicotinic ligands but the 3-phenyl-substituted derivative **6c**, which was able to discriminate the two receptor subtypes under study. This derivative displayed a moderate affinity for the α7 subtype (K_i = 0.70 μM) and lacked any affinity for the α4β2 nAChRs.

The binding data obtained on the α3β4 nAChRs showed that the tested compounds are low affinity ligands at this subtype, with K_i values in the range 6.60 μM (**6c**) and 91 μM (**5b**). As a consequence, the best α7 nAChR ligands in the set of analogues, i.e. **3a**, **3b** and **6c**, display a certain degree of subtype selectivity vs. both investigated heteromeric α/β-containing nAChRs.

Three of the studied compounds, i.e. **3a**, **5b** and **6c**, were assayed in electrophysiological experiments to assess their functional profile at the α7 nAChR subtype. Bromo-isoxazoline **3a** evoked inward whole-cell currents when applied on GH4C1 cells transfected with human α7 cDNA, clamped at −70 mV (Fig. 3a). The dose–response relationship indicated an EC_{50} value of 84.1 ± 0.8 μM, with a mean maximal amplitude which was 76 ± 5% of the mean current amplitude elicited by ACh 1 mM (n = 8, Fig. 3b). By contrast, derivatives **5b** and **6c** were able to elicit α7-mediated inward currents only when applied at the concentration of 1 mM, with a mean amplitude reaching 7 ± 4% and 26 ± 6% of that evoked by ACh 1 mM, respectively (n = 8 and n = 12, Fig. 3b). These results indicate that the 3-bromo-derivative **3a** retains the agonistic pharmacological profile of its higher homologue **1a** [12b] whereas the 3-OMe-isoxazoline **5b** and the 3-Ph-isoxazoline **6c** behave as partial agonists with different levels of potency.

4. Molecular modeling studies

With the aim of rationalizing the pharmacological results of this study, we performed a conformational analysis on the group of methoxy derivatives, which allowed to ascertain that the congeners **1**–**4** assume only one rigid boat conformation. Conversely, their analogues **5**–**7** exist as two chair conformers, one of which is

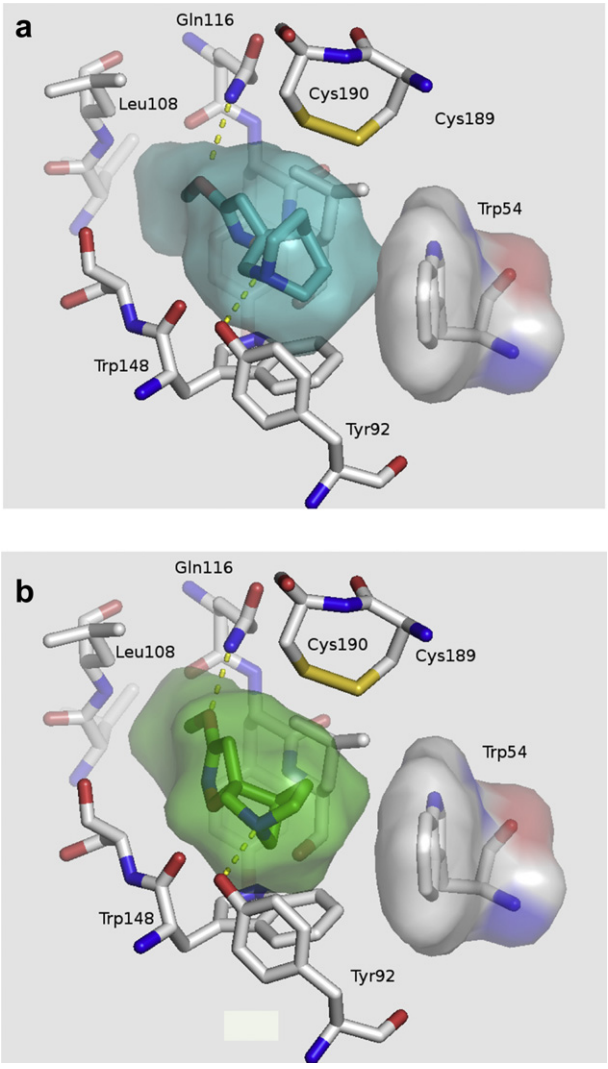

Fig. 2. Binding modes of a) (*R*)-**1b** and b) (*R*)-**3b** in the active site of the α7 nAChR subtype, after energy minimization of the complexes. Receptor model residues are depicted as stick model and carbon atoms are colored in white; surfaces and carbon atoms are colored in cyan for (*R*)-**1b** and in green for (*R*)-**3b**. Some receptor's residues have been omitted for clarity.

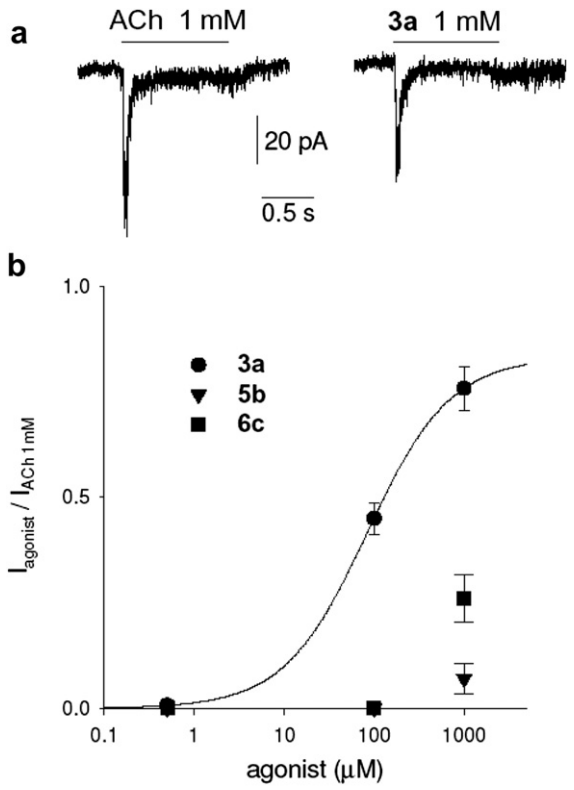

Fig. 3. a) Typical traces evoked by ACh (1 mM) or compound **3a** (1 mM) on GH4C1 cells stably transfected with human α7 nAChR subunit. b) Dose-normalized response relationships of derivatives **3a**, **5b**, and **6c** at human α7 nAChRs.

dominating, i.e. 99% populated in the case of **7a**. Thus, spirocyclic derivatives **1**–**4** may be viewed as 3-substituted piperidines forced in a boat conformation by insertion of a bridge formed by one or two methylene groups. We superimposed the eutomer (*R*)-**1a** [12b] with the two conformers of (*S*)-**7a**. We chose enantiomer (*S*)-**7a** since it shares with (*R*)-**1a** the same spatial arrangement of the substituents around the stereogenic center. The basic moiety of the favored conformer of (*S*)-**7a** (represented in white in Fig. 1, Supporting Information) overlapped perfectly with that of the (*R*)-**1a** conformer, while the two spirocyclic rings assumed different spatial orientations. On the contrary, the isoxazoline rings of (*R*)-**1a** and the lowest populated conformer of (*S*)-**7a** (represented in green in Fig. 1, Supporting Information) could be superimposed whereas their basic nitrogen atoms did not fit. The poor overall superimposition of both conformers of (*S*)-**7a** with (*R*)-**1a** may account for the low affinity showed by ligands **5a**–**c** and **7a**–**c** when compared to the corresponding quinuclidine-containing model compounds.

Another result which deserves further analysis is the drop in affinity observed on passing from the two agonists **1a** and **1b** to their congeners **3a** and **3b**. These derivatives share the boat conformation of the piperidine-like basic moiety and the agonist functional profile, as we proved for the couple **1a** and **3a**. To rationalize the biological results we used the molecular model of the α7 nAChR subtype elaborated by our research group [18], and performed docking calculations on (*R*)-**1b** [12b] and (*R*)-**3b**, the putative eutomer. We found that the best pose obtained with (*R*)-**3b** gave rise to the same polar contacts observed with (*R*)-**1b**, i.e., two hydrogen bonding with the side chains of Gln116 and Tyr92 (Fig. 2). However, at variance with what we could predict from the 2D structures of **1b** and **3b**, the basic moieties showed some differences in their binding to the α7 nAChR. In fact, we found that the bicyclic ring of (*R*)-**3b** created weaker contacts with the aromatic box which characterizes the α7 subtype binding cleft [12b], and, in particular, the cation-π interaction with the side chain of Trp54 was totally missing (Fig. 2b). Moreover, a steric clash between the Δ^2-isoxazoline moiety of (*R*)-**3b** and the backbone of Trp148, proved by its relaxation during the energy minimization of the complex, further worsened the overall quality of the binding mode of this ligand. These findings may help explaining the parallel reduction of the affinity showed by **3b** and **3a** in comparison with **1b** and **1a**, respectively.

5. Conclusion

In summary, the quinuclidine nucleus in the series of spirocyclic derivatives under study maximizes their molecular interaction with the α7 subtype, thus providing ligands with both relevant binding affinity and functional discrimination toward the α4β2 subtype. A progressive decrease in the α7 binding affinity has been detected on passing from quinuclidines to 1-azabicyclo[2.2.1]heptanes, and to *N*-methylpiperidines or piperidines. We found that the inability of these simplified analogues to retain the α7 affinity/selectivity profile of the model structures has to be attributed to a decrease of the complementary fit within the binding cleft of the α7 receptor protein and, for the *N*-methylpiperidine or piperidine derivatives, to the loss of suitable conformational requirements. In terms of functional profile, electrophysiological assays suggest a comparable α7-mediated activation pattern for **3a** and **1a**, i.e. the homologues having a dimethylene or a monomethylene bridge. The lack of this structural fragment causes a meaningful reduction of the functional response at the α7 subtype, as it has been observed for derivatives **5b** and **6c**.

6. Experimental protocols

6.1. Chemistry

^{1}H NMR and ^{13}C NMR spectra were recorded with a Varian Mercury 300 (^{1}H, 300.063; ^{13}C, 75.451 MHz) spectrometer in $CDCl_3$ solutions (unless otherwise indicated) at 20 °C. Chemical shifts (δ) are expressed in ppm and coupling constants (J) in Hz. TLC analyses were performed on commercial silica gel 60 F_{254} aluminum sheets; spots were further evidenced by spraying with a dilute alkaline potassium permanganate solution or, for tertiary amines, with the Dragendorff reagent. Melting points were determined on a model B 540 Büchi apparatus and are uncorrected. ESI mass spectra of the final salts were obtained on a Varian 320 LC-MS/MS instrument. Data are reported as mass-to-charge ratio (m/z) of the corresponding positively charged molecular ions. Microanalyses (C, H, Br, I, N) agreed with the theoretical value within ±0.4%.

6.1.1. 1-Boranyl-1-azabicyclo[2.2.1]heptan-3-one *10*

A 1.0 M solution of borane-THF complex (10 mL) was added under nitrogen to a stirred solution of 1-azabicyclo[2.2.1]heptan-3-one **9** [13] (1.11 g, 10.0 mmol) in dry THF (20 mL) at 0 °C. After stirring for 10 min at r.t., the reaction mixture was concentrated in vacuo and the residue was purified by silica gel column chromatography (cyclohexane/ethyl acetate 7:3) to yield the *N*-boranyl ketone **10** (612 mg, 49% yield).

10: Viscous colorless oil. R_f = 0.55 (cyclohexane/ethyl acetate 1:1). ^{1}H NMR: 1.91–2.01 (m, 1H), 2.32–2.43 (m, 1H), 3.01–3.39 (m, 5H), 3.27 (dd, 1H, J = 3.9 and 17.3), 3.46 (dd, 1H, J = 2.8 and 17.3). ^{13}C NMR: 29.56, 50.49, 58.27, 59.98, 69.76, 210.25. Anal. Calcd for $C_6H_{12}BNO$ (124.98): C, 57.66; H, 9.68; N, 11.21. Found: C, 57.91; H, 9.45; N, 11.47.

*6.1.2. 1-Boranyl-3-methylene-1-azabicyclo[2.2.1]heptane **11***

To an ice-bath cooled suspension of *tert*-BuOK (754 mg, 6.72 mmol) in anhydrous THF (25 mL), methyl triphenylphosphonium bromide (2.43 g, 7.20 mmol) was added. After 15 min, the reaction mixture was heated at reflux for 45 min. After cooling, a solution of **10** (600 mg, 4.80 mmol) in anhydrous THF (3 mL) was added and the mixture was stirred at r.t. for 1 h. Then, the reaction was quenched with acetone (8 mL) and the solid was filtered off. The liquid phase was concentrated under reduced pressure and the crude mixture was purified by silica gel column chromatography (cyclohexane/EtOAc 95:5) to afford alkene **11** (573 mg, 97% yield).

11: Thick pale yellow oil. $R_f = 0.43$ (cyclohexane/ethyl acetate 4:1). ^{1}H NMR: 1.66–1.75 (m, 1H), 2.06–2.17 (m, 1H), 2.78–2.96 (m, 3H), 3.10–3.21 (m, 2H), 3.40 (dd, 1H, $J = 2.2$ and 15.8), 3.63 (dd, 1H, $J = 2.6$ and 15.8), 4.75 (d, 1H, $J = 2.6$), 4.99 (d, 1H, $J = 2.6$). ^{13}C NMR: 30.92, 45.12, 59.90, 66.30, 67.01, 104.35, 147.93; Anal. Calcd for $C_7H_{14}BN$ (123.00): C, 68.35; H, 11.47; N, 11.39. Found: C, 68.73; H, 11.21; N, 11.67.

*6.1.3. 3-Bromo-1-oxa-2,7-diaza-7-boranyl-7,9-methanospiro[4.5]dec-2-ene **12a***

To a suspension of **11** (500 mg, 4.07 mmol) and $NaHCO_3$ (4.45 g, 52.91 mmol) in ethyl acetate (30 mL) was added dibromoformaldoxime (907 mg, 4.47 mmol). The reaction mixture was stirred at room temperature for 2 days, then Celite® was added, and the resulting slurry was filtered under vacuum and washed with ethyl acetate. The solvent was evaporated and the residue was column chromatographed (cyclohexane/ethyl acetate 4:1) to afford compound **12a** (876 mg, 88% yield).

12: yellow oil: $R_f = 0.47$ (cyclohexane/ethyl acetate 1:4). ^{1}H NMR: 1.59–1.69 (m, 1H), 2.02–2.14 (m, 1H), 2.80 (d, 1H, $J = 4.8$), 2.86–2.94 (m, 2H), 3.09 (dd, 1H, $J = 2.6$ and 13.6), 3.17 (d, 1H, $J = 17.8$), 3.15–3.32 (m, 2H), 3.33 (d, 1H, $J = 17.8$), 3.47 (dd, 1H, $J = 2.6$ and 13.6). ^{13}C NMR: 23.68, 45.68, 45.94, 58.39, 64.47, 71.61, 92.48, 137.26; Anal. Calcd for $C_8H_{14}BBrN_2O$ (244.92): C, 39.23; H, 5.76; N, 11.44. Found: C, 39.50; H, 5.47; N, 11.26.

*6.1.4. 3-Methoxy-1-oxa-2,7-diaza-7-boranyl-7,9-methanospiro[4.5]dec-2-ene **12b***

A stirred suspension of bromo-Δ^2-isoxazoline **12a** (485 mg, 1.98 mmol) and K_2CO_3 (2.74 g, 19.80 mmol) in methanol (30 mL) was stirred at reflux for 4 h. After addition of Celite® and filtration under vacuum, the crude filtrate was submitted to a silica gel column chromatography (cyclohexane/ethyl acetate 1:1), which gave the title compound **12b** (373 mg, 96% yield).

12b: Colorless viscous oil. $R_f = 0.40$ (cyclohexane/ethyl acetate 1:4). ^{1}H NMR: 1.63–1.72 (m, 1H), 2.03–2.15 (m, 1H), 2.80–3.21 (m, 4H), 3.08 (dd, 1H, $J = 2.5$ and 13.5), 2.97 (d, 1H, $J = 16.5$), 3.11 (d, 1H, $J = 16.5$), 3.28 (m, 1H), 3.46 (dd, 1H, $J = 2.5$ and 13.5), 3.85 (s, 3H). ^{13}C NMR: 23.83, 36.93, 45.65, 57.35, 58.35, 64.12, 71.67, 91.38, 166.97. Anal. Calcd for $C_9H_{17}BN_2O_2$ (196.05): C, 55.14; H, 8.74; N, 14.29. Found: C, 55.39; H, 8.87; N, 14.02.

*6.1.5. 3-Bromo-1-oxa-2,7-diaza-7,9-methanospiro[4.5]dec-2-ene **13a***

To an ice-bath cooled and stirred solution of **12a** (316 mg, 1.29 mmol) in acetone (10 mL) at 0 °C, trifluoroacetic acid (0.67 mL, 9.03 mmol) was added dropwise and the mixture was stirred at r.t. for 10 h. After concentration at reduced pressure, the residue was dissolved in water (10 mL) and treated with ether (3 × 5 mL). The residual aqueous phase was made alkaline by portionwise addition of solid K_2CO_3 (pH = 10) and extracted with dichloromethane (3 × 5 mL). The combined organic phases were dried over anhydrous Na_2SO_4, concentrated under reduced pressure, and the crude residue was purified by silica gel column chromatography (dichloromethane/methanol 95:5) to afford the free amine **13a** (194 mg, 65% yield).

13a: Yellow oil. $R_f = 0.14$ (dichloromethane/methanol 9:1). ^{1}H NMR: 1.19–1.28 (m, 1H), 1.53–1.65 (m, 1H), 2.33–2.42 (m, 2H), 2.50–2.57 (m, 2H), 2.69–2.80 (m, 1H), 2.84 (m, 1H), 3.00 (d, 1H, $J = 17.6$), 3.12 (dd, 1H, $J = 2.0$ and 13.5), 3.32 (d, 1H, $J = 17.6$). ^{13}C NMR: 24.15, 45.57, 46.91, 53.61, 59.84, 69.63, 94.69, 136.37. Anal. Calcd for $C_8H_{11}BrN_2O$ (231.09): C, 41.58; H, 4.80; N, 12.12. Found: C, 41.26; H, 5.09; N, 12.37.

*6.1.6. 3-Methoxy-1-oxa-2,7-diaza-7,9-methanospiro[4.5]dec-2-ene **13b***

Intermediate **12b** (370 mg, 1.89 mmol) was reacted following the protocol above described for the preparation of **13a**, which afforded the free amine **13b** (179 mg, 52% yield).

13b: Light yellow oil. $R_f = 0.29$ (dichloromethane/methanol 9:1). ^{1}H NMR: 1.10–1.20 (m, 1H), 1.43–1.54 (m, 1H), 2.23 (dd, 1H, $J = 3.0$ and 9.9), 2.26–2.33 (m, 1H), 2.42 (dd, 1H, $J = 3.0$ and 13.2), 2.49 (d, 1H, $J = 4.7$), 2.60–2.70 (m, 1H), 2.70 (d, 1H, $J = 16.8$), 2.76 (dd, 1H, $J = 1.7$ and 9.9), 2.98 (dd, 1H, $J = 2.2$ and 13.2), 2.99 (d, 1H, $J = 16.8$), 3.67 (s, 3H). ^{13}C NMR: 24.36, 36.71, 46.61, 53.58, 56.94, 59.43, 69.38, 93.41, 167.01. Anal. Calcd for $C_9H_{14}N_2O_2$ (182.22): C, 59.32; H, 7.74; N, 15.37. Found: C, 59.56; H, 7.48; N, 15.11.

*6.1.7. 3-Phenyl-1-oxa-2,7-diaza-7,9-methanospiro[4.5]dec-2-ene **13c***

A 3.5% aqueous solution of NaClO (9.7 mL, 4.56 mmol) was added dropwise to a solution of dipolarophile **11** (561 mg, 4.56 mmol) in dichloromethane (15 mL) and benzaldoxime (552 mg, 4.56 mmol). After stirring for 10 h at r.t., further 1.5 equiv of benzaldoxime and NaClO were added. The reaction mixture was further stirred for 3 h, then poured into water (10 mL) and the aqueous phase was extracted with dichloromethane (3 × 10 mL). The pooled organic extracts were dried over anhydrous Na_2SO_4 and the residue was purified by silica gel column chromatography providing cycloadduct **13c** (94 mg, 9% yield).

13c: Yellow oil. $R_f = 0.25$ (dichloromethane/methanol 9:1). ^{1}H NMR: 1.41–1.50 (m, 1H), 1.64–1.73 (m, 1H), 2.46–2.58 (m, 2H), 2.62–2.68 (m, 2H), 2.82–2.91 (m, 1H), 3.04 (m, 1H), 3.20 (d, 1H, $J = 17.1$), 3.27 (dd, 1H, $J = 2.2$ and 11.6), 3.54 (d, 1H, $J = 17.1$), 7.34–7.43 (m, 3H), 7.61–7.66 (m, 2H). ^{13}C NMR: 24.19, 45.43, 46.67, 57.61, 61.87, 67.47, 94.35, 126.65, 128.59, 130.07, 156.35. Anal. Calcd for $C_{14}H_{16}N_2O$ (228.29): C, 73.66; H, 7.06; N, 12.27. Found: C, 73.92; H, 7.15; N, 12.03.

*6.1.8. tert-Butyl-3-bromo-1-oxa-2,7-diazaspiro[4.5]dec-2-ene-7-carboxylate **16a***

The pericyclic reaction was performed on dipolarophile **15** (3.0 g, 15.21 mmol) following the protocol above reported for olefin **12a**. The crude reaction mixture was purified by column chromatography (petroleum ether/ethyl acetate 9:1) to afford cycloadduct **16a** (4.66 g, 96% yield).

16a: Crystallized from *n*-hexane as a colorless powder, mp 93–95 °C. $R_f = 0.23$ (petroleum ether/ethyl acetate 9:1). ^{1}H NMR (DMSO-d_6): 1.38 (s, 9H), 1.41–1.48 (m, 1H), 1.59–1.71 (m, 1H), 1.79–1.84 (m, 2H), 3.00 (d, 1H, $J = 17.3$), 3.11 (d, 1H, $J = 17.3$), 3.19–3.28 (m, 1H), 3.30–3.36 (m, 1H), 3.31 (d, 1H, $J = 13.0$), 3.40 (d, 1H, $J = 13.0$). ^{13}C NMR: 23.24, 28.56, 34.68, 43.17, 49.51, 50.96, 80.37, 85.65, 136.95, 154.86. Anal. Calcd for $C_{12}H_{19}BrN_2O_3$ (319.19): C, 45.15; H, 6.00; N, 8.78. Found: C, 45.27; H, 6.07; N, 8.64.

*6.1.9. tert-Butyl-3-methoxy-1-oxa-2,7-diazaspiro[4.5]dec-2-ene-7-carboxylate **16b***

Compound **16a** (1.0 g, 3.13 mmol) was reacted following the protocol previously described for **12b**. The title methoxy derivative

16b was isolated (813 mg, 96% yield) by silica gel column chromatography.

16b: Yellow oil. $R_f = 0.32$ (petroleum ether/ethyl acetate 4:1). ^{1}H NMR: 1.38 (s, 9H), 1.71–1.82 (m, 4H), 2.59–2.73 (m, 2H), 2.92–3.10 (m, 2H), 3.62–3.68 (m, 2H), 3.77 (s, 3H). ^{13}C NMR: 23.39, 28.53, 35.03, 40.66, 43.17, 50.94, 57.15, 80.07, 84.42, 154.94, 167.04. Anal. Calcd for $C_{13}H_{22}N_2O_4$ (270.32): C, 57.76; H, 8.20; N, 10.36. Found: C, 58.04; H, 8.47; N 10.08.

6.1.10. tert-Butyl-3-phenyl-1-oxa-2,7-diazaspiro[4.5]dec-2-ene-7-carboxylate **16c**

The title compound was prepared from dipolarophile **15** (300 mg, 1.52 mmol) following the procedure above described for **13c**. The crude reaction mixture was purified by column chromatography (petroleum ether/ethyl acetate 9:1) to afford cycloadduct **16c** (467 mg, 97% yield).

16c: Crystallized from *n*-hexane/EtOAc (1:1) as a colorless powder, mp 162–162.5 °C. $R_f = 0.43$ (petroleum ether/ethyl acetate 4:1). ^{1}H NMR (DMSO-d_6): 1.37 (s, 9H), 1.47–1.54 (m, 1H), 1.69–1.76 (m, 1H), 1.82–1.87 (m, 2H), 3.13 (m, 2H), 3.35 (m, 4H), 7.43–7.44 (m, 3H), 7.62–7.64 (m, 2H). ^{13}C NMR: 23.55, 28.57, 28.64, 35.09, 43.12, 51.49, 80.18, 84.69, 126.73, 128.92, 130.04, 130.30, 155.05, 156.38. Anal. Calcd for $C_{18}H_{24}N_2O_3$ (316.39): C, 68.33; H, 7.65; N, 8.85. Found: C, 68.53; H, 7.70; N, 8.69.

6.1.11. 3-Bromo-1-oxa-2,7-diazaspiro[4.5]dec-2-ene **17a**

To a stirred ice cooled solution of cycloadduct **16a** (400 mg, 1.25 mmol) in dioxane (3 mL) was added a 4N HCl solution in dioxane (0.5 mL, 2 mmol). The reaction mixture was then stirred at r.t. for about 1 h (TLC monitoring). The solvent was removed in vacuo and a saturated $NaHCO_3$ aqueous solution (about 8 mL) was added (pH = 8), which was extracted with ether (5 × 5 mL). The pooled organic extracts were dried over anhydrous Na_2SO_4 and the crude residue was purified by silica gel column chromatography (dichloromethane/methanol 98:2) to provide the tertiary base **17a** (187 mg, 68% yield).

17a: Yellow oil. $R_f = 0.24$ (dichloromethane/methanol 95:5). ^{1}H NMR: 1.45–1.57 (m, 1H), 1.73–1.83 (m, 1H), 1.92–1.98 (m, 2H), 2.46 (d, 1H, $J = 16.0$), 2.56 (d, 1H, $J = 16.0$), 2.70–2.78 (m, 1H), 2.89 (d, 1H, $J = 17.3$), 2.94–2.96 (m, 1H), 3.02 (d, 1H, $J = 17.3$). ^{13}C NMR (DMSO-d_6): 23.85, 29.90, 34.67, 45.38, 50.45, 85.40, 137.14. Anal. Calcd for $C_7H_{11}BrN_2O$ (219.08): C, 38.38; H, 5.06; N, 12.79. Found: C, 38.63; H, 4.88; N, 12.57.

6.1.12. 3-Methoxy-1-oxa-2,7-diazaspiro[4.5]dec-2-ene **17b**

The protected amine **16b** (400 mg, 1.48 mmol) was reacted following the protocol previously described for the preparation of the **13a**. Secondary amine **17b** was obtained (219 mg, 87% yield) by silica gel column chromatography,

17b: Thick yellow oil. $R_f = 0.46$ (dichloromethane/methanol 95:5). ^{1}H NMR: 1.46–1.53 (m, 1H), 1.70–1.80 (m, 2H), 1.89–1.94 (m, 1H), 2.64–2.76 (m, 4H), 2.79–2.87 (m, 1H), 2.89–2.94 (m, 1H), 3.83 (s, 3H). ^{13}C NMR: 24.19, 34.93, 41.56, 45.68, 54.41, 56.96, 83.93, 167.13; Anal. Calcd for $C_8H_{14}N_2O_2$ (170.21): C, 56.45; H, 8.29; N, 16.46. Found: C, 56.21; H, 8.52; N, 16.68.

6.1.13. 3-Phenyl-1-oxa-2,7-diazaspiro[4.5]dec-2-ene **17c**

The protected amine **16c** (430 mg, 1.36 mmol) was reacted following the protocol previously described for the preparation of the **13a**. Secondary amine **17c** (273 mg, 93% yield) was purified by silica gel column chromatography.

17c: Thick light yellow oil. $R_f = 0.52$ (dichloromethane/methanol 9:1). ^{1}H NMR: 1.57–1.64 (m, 1H), 1.78–1.90 (m 2H), 1.96–2.02 (m, 1H), 2.73–2.82 (m, 1H), 2.80 (d, 1H, $J = 13.0$), 2.86–2.92 (m, 1H), 2.96 (d, 1H, $J = 13.0$), 3.00 (d, 1H, $J = 16.8$), 3.16 (d, 1H, $J = 16.8$), 7.37–7.42 (m, 3 H), 7.63–7.68 (m, 2H). ^{13}C NMR: 24.61, 35.16, 43.87, 44.00, 45.84, 54.77, 84.51, 126.64, 128.85, 130.15, 156.46. Anal. Calcd for $C_{13}H_{16}N_2O$ (216.28): C, 72.19; H, 7.46; N, 12.95. Found: C, 72.42; H, 7.21; N, 12.77.

6.1.14. 3-Bromo-7-methyl-1-oxa-2,7-diazaspiro[4.5]dec-2-ene **18a**

A 37% aqueous solution of formaldehyde (0.628 mL, 8.4 mmol) and $NaBH_3CN$ (211 mg, 3.36 mmol) were added portionwise to a stirred solution of **17a** (370 mg, 1.69 mmol) in CH_3CN (10 mL). After stirring at r.t. for 20 min, the solvent was removed, and the residue was partitioned between dichloromethane and acidic water (pH = 3). The residual aqueous phase (about 10 mL), after addition of solid $NaHCO_3$ (pH = 8), was extracted with dichloromethane (3 × 5 mL). The combined organic extracts were dried over anhydrous Na_2SO_4, concentrated in vacuo, and column chromatographed to afford the tertiary amine **18a** (360 mg, 92% yield).

18a: Yellow oil. $R_f = 0.58$ (dichloromethane/methanol 9:1). ^{1}H NMR: 1.41–2.60 (m, 1H), 1.60–1.68 (m, 2H), 1.68–1.86 (m, 1H), 2.14–2.20 (m, 2H), 2.20–2.60 (m, 2H), 2.24 (s, 3H), 2.89 (d, 1H, $J = 17.5$), 3.06 (d, 1H, $J = 17.5$). ^{13}C NMR: 22.95, 34.01, 46.40, 47.78, 54.92, 63.23, 86.99, 148.47. Anal. Calcd for $C_8H_{13}BrN_2O$ (233.11): C, 41.22; H, 5.62; N, 12.02. Found: C, 41.47; H, 5.85; N, 11.79.

6.1.15. 3-Methoxy-7-methyl-1-oxa-2,7-diazaspiro[4.5]dec-2-ene **18b**

The secondary amine **17b** (236 mg, 1.39 mmol) was reacted following the procedure above described for the preparation of **18a**. Tertiary amine **18b** was isolated (243 mg, 95% yield) by silica gel column chromatography.

18b: Light yellow oil. $R_f = 0.62$ (dichloromethane/methanol 9:1). ^{1}H NMR: 1.50–1.62 (m, 1H), 1.63–175 (m, 2H), 1.76–1.84 (m, 1H), 2.05–2.18 (m, 1H), 2.19–2.27 (m, 1H), 2.28 (s, 3H), 2.50–2.67 (m, 2H), 2.72 (d, 1H, $J = 16.5$), 2.95 (d, 1H, $J = 16.5$), 3.83 (s, 3H). ^{13}C NMR: 23.08, 34.04, 41.62, 46.27, 55.02, 56.64, 63.41, 84.79, 166.80. Anal. Calcd for $C_9H_{16}N_2O_2$ (184.24): C, 58.67; H, 8.75; N, 15.21. Found: C, 58.52, H, 9.03, N, 14.98.

6.1.16. 3-Phenyl-7-methyl-1-oxa-2,7-diazaspiro[4.5]dec-2-ene **18c**

The secondary amine **17c** (200 mg, 0.92 mmol) was reacted following the procedure above described for the preparation of **18a**. Tertiary amine **18c** was isolated (192 mg, 90% yield) by silica gel column chromatography.

18c: Light yellow oil. $R_f = 0.27$ (dichloromethane/methanol 9:1). ^{1}H NMR: 1.55–1.63 (m, 1H), 1.72–1.82 (m, 2H), 1.85–1.90 (m, 1H), 2.10–2.22 (m, 1H), 2.23–2.38 (m, 1H), 2.31 (s, 3H), 2.50–2.68 (m, 2H), 3.06 (d, 1H, $J = 16.7$), 3.35 (d, 1H, $J = 16.7$), 7.37–7.40 (m, 3H), 7.65–7.68 (m, 2H). ^{13}C NMR: 23.52, 34.31, 44.34, 46.62, 55.32, 63.77, 85.41, 126.71, 128.85, 130.08, 130.25, 156.40. Anal. Calcd for $C_{14}H_{18}N_2O$ (230.31): C, 73.01; H, 7.88; N, 12.16. Found: C, 73.40; H, 7.64; N, 11.91.

6.1.17. General procedure for the preparation of fumarates

To a solution of the free base (0.8 mmol) in methanol (3 mL) was added a solution of fumaric acid (102 mg, 0.88 mmol) in methanol (2 mL). After stirring overnight at room temperature, the solvent was removed at reduced pressure and the crude fumarate, which was obtained quantitatively, was crystallized.

3-Bromo-1-oxa-2,7-diaza-7,9-methanospiro[4.5]dec-2-ene fumarate ***3a*** × ***3/4 $C_4H_4O_4$***: Crystallized from 2-propanol as colorless prisms, mp 169–170 °C. ^{1}H NMR (CD_3OD): 1.74–1.84 (m, 1H), 2.06–2.18 (m, 1H), 2.97 (d, 1H, $J = 5.0$), 3.10–3.19 (m, 1H), 3.24 (dd, 1H, $J = 2.5$ and 9.5), 3.29–3.45 (m, 2H), 3.45 (d, 1H, $J = 18.2$), 3.45 (dd, 1H, $J = 2.8$ and 13.0), 3.62 (d, 1H, $J = 18.2$), 3.65 (dd, 1H, $J = 2.8$ and 13.0), 6.69 (s, 1.5H). ^{13}C NMR (CD_3OD): 21.31, 45.01, 51.67, 58.65, 64.93, 65.74, 91.25, 135.02, 138.06, 169.80. MS (ESI) *m/z* $[M]^+$ Calcd for $C_8H_{11}BrN_2O$: 231.1. Found: 231.0. Anal. Calcd for $C_{11}H_{14}BrN_2O_4$

(318.14): C, 41.53; H, 4.44; Br, 25.12; N, 8.81. Found: C, 41.77; H, 4.23; Br, 24.86; N, 8.58.

3-Methoxy-1-oxa-2,7-diaza-7,9-methanospiro[4.5]dec-2-ene fumarate ***3b*** × ***1/2 $C_4H_4O_4$***: Crystallized from 2-propanol as colorless prisms, mp 149–150 °C. ^{1}H NMR (CD_3OD): 1.75–1.87 (m, 1H), 2.08–2.27 (m, 1H), 2.86–3.10 (m, 2H), 3.15–3.38 (m, 2H), 3.39–3.58 (m, 2H), 3.61–3.77 (m, 2H), 3.83 (s, 3H); 3.90–4.07 (m, 1H), 6.70 (s, 1H). ^{13}C NMR (CD_3OD): 21.40, 24.26, 44.80, 56.75, 58.43, 63.63, 64.92, 65.73, 134.63, 167.72, 168.58. MS (ESI) *m/z* $[M + H]^+$ Calcd for $C_9H_{14}N_2O_2$: 182.2. Found: 183.1. Anal. calcd for $C_{11}H_{16}N_2O_4$ (240.26): C, 54.99; H, 6.71; N, 11.66. Found: C, 55.18; H, 6.53; N, 11.79.

3-Phenyl-1-oxa-2,7-diaza-7,9-methanospiro[4.5]dec-2-ene fumarate ***3c*** × ***1/2 $C_4H_4O_4$***: Crystallized from 2-propanol as colorless prisms, mp 176.5–177.5 °C. ^{1}H NMR (CD_3OD): 1.80–1.90 (m, 1H), 2.06–2.18 (m, 1H), 2.97 (d, 1H, $J = 4.7$), 3.16–3.22 (m, 1H), 3.25 (dd, 1H, $J = 2.3$ and 9.6), 3.30–3.44 (m, 1H), 3.44–3.58 (m, 2H), 3.54 (d, 1H, $J = 17.8$), 3.68–3.77 (m, 1H), 3.73 (d, 1H, $J = 17.8$), 6.53 (s, 1H), 7.34–7.41 (m, 3H), 7.54–7.57 (m, 2H). ^{13}C NMR (CD_3OD):0.21.34, 45.13, 51.55, 58.78, 65.06, 65.66, 91.65, 128.21, 128.86, 130.27, 131.03, 134.55, 156.22, 168.76. MS (ESI) *m/z* $[M + H]^+$ Calcd for $C_{14}H_{16}N_2O$: 228.3. Found: 229.1. Anal. Calcd for $C_{16}H_{18}N_2O_3$ (286.33): C, 67.12; H, 6.34; N, 9.78. Found: C, 67.35; H, 6.39; N, 10.02.

3-Bromo-7-methyl-1-oxa-2,7-diazaspiro[4.5]dec-2-ene fumarate ***5a*** × ***3/4 $C_4H_4O_4$***: Crystallized from 2-propanol as pale yellow prisms, mp 121–122 °C dec. ^{1}H NMR (D_2O): 1.65–1.80 (m, 1H), 1.80–1.90 (m, 2H), 1.90–2.21 (m, 1H), 2.75 (s, 3H), 2.79–2.90 (m, 1H), 3.00–3.30 (m, 3H), 3.32–3.45 (m, 1H), 3.48–3.65 (m, 1H), 6.54 (s, 1.5H). ^{13}C NMR (CD_3OD): 24.43, 31.35, 43.54, 53.28, 58.75, 63.57, 84.68, 135.32, 149.63, 170.40; MS (ESI) *m/z* $[M]^+$ Calcd for $C_8H_{13}BrN_2O$: 233.1. Found: 233.1. Anal. Calcd for $C_{11}H_{16}BrN_2O_4$ (320.16): C, 41.27; H, 5.04; Br, 24.96; N, 8.75. Found: C, 41.38; H, 4.92; Br, 25.22; N, 8.89.

3-Methoxy-7-methyl-1-oxa-2,7-diazaspiro[4.5]dec-2-ene fumarate ***5b*** × ***3/4 $C_4H_4O_4$***: Crystallized from 2-propanol as colorless prisms, mp 136.5–137.5 °C dec. ^{1}H NMR (D_2O): 1.62–1.78 (m, 1H), 1.78–1.95 (m, 2H), 1.95–2.05 (m, 1H), 2.74 (s, 3H), 2.80–2.90 (m, 2H), 2.90–3.02 (m, 2H), 3.30–3.38 (m, 1H), 3.49–3.56 (m, 1H), 3.70 (s, 3H), 6.54 (s, 1.5H). ^{13}C NMR (CD_3OD): 29.66, 31.00, 40.89, 53.42, 56.79, 58.87, 82.38, 92.82, 135.09, 167.82, 170.05. MS (ESI) *m/z* $[M + H]^+$ Calcd for $C_9H_{16}N_2O_2$: 184.2. Found: 185.1. Anal. Calcd for $C_{12}H_{19}N_2O_5$ (271.29): C, 53.13; H, 7.06; N, 10.33. Found: C, 53.27; H, 7.26; N, 10.15.

3-Phenyl-7-methyl-1-oxa-2,7-diazaspiro[4.5]dec-2-ene fumarate ***5c*** × ***3/4 $C_4H_4O_4$***: Crystallized from 2-propanol as colorless prisms, mp 171.5–172.5 °C dec. ^{1}H NMR (D_2O): 1.78–2.02 (m, 4H), 2.75 (s, 3H), 2.84–2.94 (m, 1H), 3.06–3.10 (m, 1H), 3.29 (bs, 2H), 3.38–3.50 (m, 2H), 6.51 (s, 1.5H), 7.30–7.48 (m, 3H), 7.50–7.59 (m, 2H). ^{13}C NMR (CD_3OD): 24.15, 31.14, 43.75, 53.52, 59.16, 63.60, 82.51, 126.71, 128.78, 129.17, 130.52, 134.73, 157.57, 169.01. MS (ESI) *m/z* $[M + H]^+$ Calcd for $C_{14}H_{18}N_2O$: 230.3. Found: 231.1. Anal. Calcd for $C_{17}H_{21}N_2O_4$ (317.36): C, 64.34; H, 6.67; N, 8.83. Found: C, 64.57; H, 6.72; N, 8.65.

3-Bromo-1-oxa-2,7-diazaspiro[4.5]dec-2-ene fumarate ***7a*** × ***1/2 $C_4H_4O_4$***: Crystallized from 2-propanol/diethyl ether (1:1) as colorless needles, mp 161.5–164 °C. ^{1}H NMR (D_2O): 1.77–1.92 (m, 3H), 2.03–2.07 (m, 1H), 2.86–2.94 (m, 1H), 3.05–3.15 (m, 3H), 3.26–3.30 (m, 1H), 3.40–3.46 (m, 1H), 6.41 (s, 1H). ^{13}C NMR (CD_3OD): 24.20, 31.72, 46.77, 48.77, 63.61, 83.63, 134.63, 149.83, 168.69. MS (ESI) *m/z* $[M]^+$ Calcd for $C_7H_{11}BrN_2O$: 219.1. Found: 218.9. Anal. Calcd for $C_9H_{13}BrN_2O_3$ (277.12): C, 39.01; H, 4.73; Br, 28.83; N, 10.11. Found: C, 39.19; H, 4.57; Br, 28.98; N, 10.02.

3-Methoxy-1-oxa-2,7-diazaspiro[4.5]dec-2-ene fumarate ***7b*** × ***1/2 $C_4H_4O_4$***: Crystallized from 2-propanol as colorless prisms, mp 161–163.5 °C dec. ^{1}H NMR (CD_3OD): 1.75–1.89 (m, 2H), 1.94–2.08 (m, 2H), 2.89–3.06 (m, 4H), 3.18–3.24 (m, 1H), 3.31–3.37 (m, 1H), 3.83 (s, 3H), 6.63 (s, 1H). ^{13}C NMR (CD_3OD): 24.20, 37.68, 47.87, 49.08, 55.65, 64.87, 83.97, 134.49, 162.39, 168.27. MS (ESI) *m/z* $[M + H]^+$ Calcd for $C_8H_{14}N_2O_2$: 170.2. Found: 171.1. Anal. Calcd for $C_{10}H_{16}N_2O_4$ (228.25): C, 52.62; H, 7.07; N, 12.27. Found: C, 52.81; H, 7.25; N, 12.09.

3-Phenyl-1-oxa-2,7-diazaspiro[4.5]dec-2-ene fumarate ***7c*** × ***3/4 $C_4H_4O_4$***: Crystallized from 2-propanol as colorless prisms, mp 199.5–201 °C dec. ^{1}H NMR (D_2O): 1.82–1.90 (m, 3H), 1.97–2.02 (m, 1H), 2.90–2.97 (m, 1H), 3.07–3.12 (m, 1H), 3.30 (bs, 2H), 3.20–3.39 (m, 2H), 6.51 (s, 1.5H), 7.35–7.41 (m, 3H), 7.50–7.56 (m, 2H). ^{13}C NMR (CD_3OD): 23.17, 32.15, 43.26, 59.38, 63.22, 81.97, 125.31, 127.90, 129.67, 131.02, 136.13, 155.27, 169.64. MS (ESI) *m/z* $[M + H]^+$ Calcd for $C_{14}H_{18}N_2O$: 216.3. Found: 217.0. Anal. Calcd for $C_{16}H_{19}N_2O_4$ (303.33): C, 63.35; H, 6.31; N, 9.24. Found: C, 63.12; H, 6.47; N, 9.40.

6.1.18. General procedure for the preparation of iodomethylates

To a solution of the free base (0.5 mmol) in methanol (3 mL) was added iodomethane (310 μL, 5 mmol). The solution was left overnight at room temperature, then the solvent was removed at reduced pressure affording quantitatively the crude quaternary salt, which was crystallized.

3-Bromo-1-oxa-2,7-diaza-7,9-methanospiro[4.5]dec-2-ene methyl iodide ***4a***: Crystallized from 2-propanol as colorless prisms, mp 177–178 °C. ^{1}H NMR (D_2O): 1.77–1.87 (m, 1H), 2.20–2.32 (m, 1H), 3.00 (m, 1H), 3.17 (s, 3H), 3.40–3.46 (m, 3H), 3.43 (d, 1H, $J = 18.2$), 3.58 (d, 1H, $J = 18.2$), 3.58–3.61 (m, 1H), 3.71–3.82 (m, 2H). ^{13}C NMR (D_2O): 22.70, 45.21, 45.36, 62.02, 67.53, 73.81, 92.09, 100.24, 139.95. MS (ESI) *m/z* $[M]^+$ Calcd for $C_9H_{14}BrN_2O^+$: 246.1. Found: 245.0. Anal. Calcd for $C_9H_{14}BrIN_2O$ (373.03): C, 28.98; H, 3.78; Br, 21.42; I, 34.02; N, 7.51. Found: C, 28.75; H, 3.92; Br, 21.65; I, 33.85; N, 7.78.

3-Methoxy-1-oxa-2,7-diaza-7,9-methanospiro[4.5]dec-2-ene methyl iodide ***4b***: Crystallized from 2-propanol as colorless prisms, mp 167–167.5 °C. ^{1}H NMR (D_2O): 1.75–1.91 (m, 1H), 2.18–2.30 (m, 1H), 2.98 (m, 1H), 3.15 (s, 3H), 3.16 (d, 1H, $J = 17.0$), 3.27 (d, 1H, $J = 17.0$), 3.34–3.42 (m, 3H), 3.57 (m, 1H), 3.65 (dd, 1H, $J = 2.3$ and 12.9), 3.71 (s, 3H), 3.76 (dd, 1H, $J = 2.4$ and 12.9). ^{13}C NMR (D_2O): 23.30, 26.54, 45.34, 45.57, 51.02, 61.89, 67.46, 73.98, 92.25, 164.87. MS (ESI) *m/z* $[M]^+$ Calcd for $C_{10}H_{17}N_2O_2^+$: 197.3. Found: 197.1. Anal. Calcd for $C_{10}H_{17}IN_2O_2$ (324.16): C, 37.05; H, 5.29; I, 39.15; N, 8.64. Found: C, 36.86; H 5.43; I, 39.02; N, 8.59.

3-Phenyl-1-oxa-2,7-diaza-7,9-methanospiro[4.5]dec-2-ene methyl iodide ***4c***: Crystallized from 2-propanol as a light yellow powder, mp 173.5–174 °C. ^{1}H NMR (D_2O): 1.91–1.98 (m, 1H), 2.23–2.33 (m, 1H), 2.97 (m, 1H), 3.18 (s, 3H), 3.39–3.50 (m, 3H), 3.55 (d, 1H, $J = 18.0$), 3.62 (m, 1H), 3.71 (d, 1H, $J = 18.0$), 3.71–3.83 (m, 2H), 7.34–7.42 (m, 3H), 7.52–7.56 (m, 2H). ^{13}C NMR (CD_3OD): 21.27, 45.11, 50.14, 51.64, 58.65, 64.54, 65.98, 91.11, 128.20, 128.83, 130.21, 131.06, 156.20. MS (ESI) *m/z* $[M]^+$ Calcd for $C_{15}H_{19}N_2O^+$: 243.3. Found: 243.1. Anal. Calcd for $C_{15}H_{19}IN_2O$ (370.23): C, 48.66; H, 5.17; I, 34.28; N, 7.57. Found: C, 48.83; H, 5.38; I, 34.47; N, 7.45.

3-Bromo-7-methyl-1-oxa-2,7-diazaspiro[4.5]dec-2-ene methyl iodide ***6a***: Crystallized from 2-propanol as colorless prisms, mp 198.5–199.5 °C. ^{1}H NMR (D_2O): 1.65–1.75 (m, 1H), 1.79–1.94 (m, 1H), 2.00–2.19 (m, 2H), 3.08 (s, 3H), 3.13 (s, 3H), 3.12–3.29 (m, 3H), 3.37–3.49 (m, 2H), 3.70–3.75 (m, 1H). ^{13}C NMR (CD_3OD): 17.17, 22.15, 31.05, 33.46, 45.31, 54.54, 62.64, 86.65, 148.84. MS (ESI) *m/z* $[M + H]^+$ Calcd for $C_9H_{16}BrN_2O^+$: 248.1. Found: 249.2. Anal. Calcd for $C_9H_{16}BrIN_2O$ (375.04): C, 28.82; H, 4.30; Br, 21.31; I, 33.84; N, 7.47. Found: C, 29.09; H, 4.43; Br, 21.46; I, 33.69; N, 7.22.

3-Methoxy-7-methyl-1-oxa-2,7-diazaspiro[4.5]dec-2-ene methyl iodide ***6b***: Crystallized from 2-propanol as yellow prisms, mp 187–188 °C. ^{1}H NMR (D_2O): 1.60–1.75 (m, 1H), 1.76–1.92 (m, 1H),

1.98–2.16 (m, 2H), 2.85 (d, 1H, $J = 17.1$), 2.97 (d, 1H, $J = 17.1$), 3.06 (s, 3H), 3.13 (s, 3H), 3.18–3.24 (m, 1H), 3.30 (d, 1H, $J = 13.5$), 3.39–3.48 (m, 1H), 3.68 (d, 1H, $J = 13.5$), 3.72 (s, 3H). ^{13}C NMR (CD_3OD): 17.25, 30.78, 42.21, 50.54, 56.96, 61.88, 65.77, 83.11, 167.89. MS (ESI) *m/z* $[M]^+$ Calcd for $C_{10}H_{19}N_2O_2^+$: 199.3. Found: 199.1. Anal. Calcd for $C_{10}H_{19}IN_2O_2$ (326.17): C, 36.82; H, 5.87; I, 38.91; N, 8.59. Found: C, 37.04; H, 5.71; I, 39.19; N, 8.44.

3-Phenyl-7-methyl-1-oxa-2,7-diazaspiro[4.5]dec-2-ene methyl iodide ***6c***: Crystallized from 2-propanol as colorless prisms, mp 197–198 °C. ^{1}H NMR (D_2O): 1.71–1.92 (m, 2H), 2.08–2.20 (m, 2H), 3.09 (s, 3H), 3.18 (s, 3H), 3.22–3.40 (m, 3H), 3.40–3.55 (m, 2H), 3.60–3.72 (m, 1H), 7.31–7.49 (m, 3H), 7.51–7.60 (m, 2H). ^{13}C NMR (CD_3OD): 17.60, 31.26, 45.44, 56.91, 61.86, 66.29, 83.11, 126.81, 128.86, 130.64, 157.39, 167.30. MS (ESI) *m/z* $[M]^+$ Calcd for $C_{15}H_{21}N_2O^+$: 245.3. Found: 245.1. Anal. Calcd for $C_{15}H_{21}IN_2O$ (372.24): C, 48.40; H, 5.69; I, 34.09; N, 7.53. Found: C, 48.49; H, 5.82; I, 33.91; N, 7.66.

6.2. Receptor binding assays

6.2.1. Membranes binding of [^{3}H]epibatidine and [^{125}I]α-bungarotoxin

The cortex tissues were dissected, immediately frozen on dry ice and stored at −80 °C for later use. In each experiment, the cortex tissues from two rats were homogenized in 10 mL of a buffer solution [50 mM Na_3PO_4, 1 M NaCl, 2 mM ethylenediaminetetraacetic acid (EDTA), 2 mM ethylene glycol tetraacetic acid (EGTA) and 2 mM phenylmethylsulfonyl fluoride (PMSF), pH 7.4] using a potter homogenizer; the homogenates were then diluted and centrifuged at 60,000*g* for 1.5 h. The total membrane homogenization, dilution and centrifugation procedures were performed twice, then the pellets were collected, rapidly rinsed with a buffer solution (50 mM Tris–HCl, 120 mM NaCl, 5 mM KCl, 1 mM $MgCl_2$, 2.5 mM $CaCl_2$ and 2 mM PMSF, pH 7), and resuspended in the same buffer containing a mixture of 20 μg/mL of each of the following protease inhibitors: leupeptin, bestatin, pepstatin A, and aprotinin.

6.2.2. [^{3}H]Epibatidine binding

(±)-[^{3}H]Epibatidine with a specific activity of 56–60 Ci/mmol was purchased from Perkin Elmer (Boston MA); the nonradioactive α-bungarotoxin, epibatidine, and nicotine were purchased from Sigma Aldrich (Italy). It has been previously reported that [^{3}H]epibatidine also binds to α-bungarotoxin binding receptors with nM affinity [19]. In order to prevent the binding of [^{3}H]epibatidine to the α-bungarotoxin binding receptors, the membrane homogenates were pre-incubated with 2 μM α-bungarotoxin and then with [^{3}H]epibatidine. The saturation experiments were performed by incubating aliquots of cortex membrane homogenates with 0.01–2.5 nM concentrations of (±)-[^{3}H]epibatidine overnight at 4 °C. Nonspecific binding was determined in parallel by means of incubation in the presence of 100 nM unlabelled epibatidine. At the end of the incubation, the samples were filtered on a GFC filter soaked in 0.5% polyethylenimine and washed with 15 mL of a buffer solution (10 mM Na_3PO_4, 50 mM NaCl, pH 7.4), and the filters were counted in a β counter.

6.2.3. [^{125}I]α-bungarotoxin binding

The saturation binding experiments were performed using aliquots of cortex membrane homogenates incubated overnight with 0.1–10 nM concentrations of [^{125}I]α-bungarotoxin (specific activity 200–213 Ci/mmol, Amersham) at r.t. Nonspecific binding was determined in parallel by means of incubation in the presence of 1 μM unlabelled α-bungarotoxin. After incubation, the samples were filtered as described above and the bound radioactivity was directly counted in a γ counter.

6.2.4. Binding to heterologously expressed α3β4 receptors

HEK 293 cells were grown in Dulbecco's modified Eagle medium supplemented with 10% fetal bovine serum, 1% L-Glutamine, 100 units/ml penicillin G, and 100 μg/streptomycin in a humidified atmosphere containing 10% CO_2. The cDNAs encoding α3 and β4 were transfected into the HEK 293 cells at 30% confluency. The cell transfections were performed in 100 mm Petri dishes using 30 μL of JetPEI™ (Polypus, France) (1 mg/ml, pH 7.2) and 10 μg of cDNAs. After 48 h transfection, the cells were collected, washed with PBS by centrifugation, and used for binding analysis.

6.2.5. Affinity of compounds ***3a–c***, ***4a–c***, ***5a–c***, ***6a–c***, and ***7a–c*** for nAChRs

The inhibition of radioligand binding by epibatidine and the test compounds was measured by pre-incubating cortex homogenates with increasing doses (10 pM - 10 mM) of the reference nicotinic agonists, epibatidine or nicotine, and the drug to be tested for 30 min at r.t., followed by overnight incubation with a final concentration of 0.075 nM [^{3}H]epibatidine or 1 nM [^{125}I]α-bungarotoxin at the same temperatures as those used for the saturation experiments. These ligand concentrations were used for the competition-binding experiments because they are within the range of the K_D values of the ligands for the two different classes of nAChRs. For each compound, the experimental data obtained from the three saturation and three competition-binding experiments were analyzed by means of a non-linear least square procedure, using the LIGAND program as described by Munson and Rodbard [15]. The binding parameters were calculated by simultaneously fitting three independent saturation experiments and the K_i values were determined by fitting the data of three independent competition experiments. The errors in the K_D and K_i values of the simultaneous fits were calculated using the LIGAND software, and were expressed as percentage coefficients of variation (% CV). When final compound concentrations up to 100 μM did not inhibit radioligand binding, the K_i value was defined as being > 100 μM based on the Cheng and Prusoff's equation [20].

Binding to HEK 293 transfected α3β4 receptors was performed by overnight incubation at 4 °C with [^{3}H]Epi at a concentration ranging from 0.005 to 1 nM. All of the incubations were performed in a buffer containing 50 mM Tris–HCl, pH 7, 150 mM NaCl, 5 mM KCl, 1 mM $MgCl_2$, 2.5 mM $CaCl_2$, 2 mg/ml BSA. Specific ligand binding was defined as total binding minus the binding in the presence of 100 nM cold Epi. The inhibition of [^{3}H]Epi binding by compounds was measured by incubating increasing concentration of the compounds for 5 min followed by overnight incubation with 0.25 nM (in the case of the α3β4 subtype). After incubation, the membranes of HEK cells transfected with α3β4 receptors were washed seven times with ice-cold PBS, and the bound [^{3}H]Epi was then determined by means of liquid scintillation counting in a beta counter.

6.3. Electrophysiological recordings

The human α7 nAChRs were expressed by transient transfection in the rat anterior pituitary GH4C1 cell line [21]. Transient transfection was achieved by adding to each dish 1 μg of human α7 subunit cDNA, along with 4 μl of lipofectamine. All culture media were purchased from Invitrogen (Italy). Whole-cell current recordings were performed 2–3 days after plating. Recordings and data analysis were performed by using borosilicate glass patch pipette (3- to 6-MΩ tip resistance) connected to an Axopatch 200A amplifier (Axon Instruments, Foster City, CA). Data were stored on a PC computer by using PCLAMP10 software (Molecular Devices). During the recording period, the cells were bathed in the following solution (mM): 140 NaCl, 2 $CaCl_2$, 2.8 KCl, 2 $MgCl_2$, 10 Hepes/NaOH and 10 glucose; pH 7.3. The patch pipettes were filled with

a solution containing (mM): 140 CsCl, 2 MgATP, 10 Hepes/CsOH and 5 BAPTA; pH 7.3. Whole-cell capacitance and patch series resistance (5–15 MΩ) were estimated from slow transient compensations. A series resistance compensation of 85–90% was obtained in all cases. The cells were voltage-clamped at a holding potential of −70 mV and continuously perfused with a gravity-driven system using independent external tubes for the control and agonist-containing solutions. These tubes were positioned 50–100 μm from the patched cell and connected to a fast exchanger system (RSC-160, BioLogic, France). Dose-response relationships were constructed by sequentially applying different concentrations of agonists, and normalizing the obtained current amplitudes to the value obtained by applying 1 mM ACh on the same cell. For quantitative estimations of agonist actions, dose–response relationship were fitted to the Equation (1):

$$I = I_{max}\left\{[C]^{nH} / \left(EC50^{nH} + [C]^{nH}\right)\right\} \quad (1)$$

where I is the current amplitude induced by the agonist at concentration [C], I_{max} is the maximum response of the cell, nH is the Hill coefficient and EC_{50} is the concentration for which a half maximum response is induced.

6.4. Molecular modeling

The structures of the target compounds were built by GaussView 5.0 and minimized at the DFT/b3lyp/6-31g* level, as implemented in Gaussian09 package [22]. The amino groups were considered in the ionized form to better simulate the physiological conditions. The superimposition between both conformers of (*S*)-**7a** and (*R*)-**1a** was acquired by the PyMOL software [23]. Docking experiments of selected ligands in the binding site created by the chains D and E of a published model [18] of α7 nAChRs were performed by means of the program *GOLD 4.0* [24]. The receptor active-site radius was set equal to 11 Å from the indole nitrogen of Trp148 responsible for the primary ligand anchoring point. The side chain of Gln116 was not restrained during the docking calculation. The goldscore fitness function and the distribution of torsion angles were chosen as indicators of the quality of the docking results. Van der Waals and hydrogen bonding radii were set respectively at 4.0 and 3.0 Å, while genetic algorithm parameters were kept at the default value. The obtained complexes were further geometry optimized by means of the molecular mechanics method (by Tripos force field), implemented in Sybyl 8.0 [25].

Acknowledgments

This research was financially supported by the Italian Ministry of Education, University and Research (FIRB grant RBNE03H5Y to CDM and PRIN grant 20072BTSR2 to FC and MDA). The EC Neurocypres grant, the Terdismental grant n° ID 16983 SAL-50 from Regione Lombardia, the Compagnia San Paolo grant (2005-1964) to CG, and a grant from Associazione Oasi Maria SS, Troina, Italy to FC are also gratefully acknowledged.

References

[1] E.X. Albuquerque, E.F.R. Pereira, M. Alkondon, S.W. Rogers, Physiol. Rev. 89 (2009) 73–120.
[2] J.A. Dani, D. Bertrand, Annu. Rev. Pharmacol. Toxicol. 47 (2007) 699–729.
[3] a) C. Gotti, F. Clementi, Prog. Neurobiol. 74 (2004) 363–396;
b) C. Gotti, M. Zoli, F. Clementi, Trends Pharmacol. Sci. 27 (2006) 482–491.
[4] A.A. Jensen, B. Frølund, T. Liljefors, P. Krogsgaard-Larsen, J. Med. Chem. 48 (2005) 4705–4745.
[5] a) E. Shearman, S. Rossi, H. Sershen, A. Hashim, A. Lajtha, Neurochem. Res. 30 (2005) 1055–1066;
b) J. Barik, S. Wonnacott, Mol. Pharmacol. 69 (2006) 618–628.
[6] a) F. Dajas-Bailador, S. Wonnacott, Trends Pharmacol. Sci. 25 (2004) 317–324;
b) S. Fucile, Cell Calcium 35 (2004) 1–8.
[7] a) M.N. Romanelli, P. Gratteri, L. Guandalini, E. Martini, C. Bonaccini, F. Gualtieri, ChemMedChem 2 (2007) 746–767;
b) S.L. Cincotta, M.S. Yorek, T.M. Moschak, S.R. Lewis, J.S. Rodefer, Curr. Opin. Invest. Drugs 9 (2008) 47–56;
c) A. Taly, P.J. Corringer, D. Guedin, P. Lestage, J.P. Changeux, Nat. Rev. Drug Discov. 8 (2009) 733–750.
[8] a) W.J. de Jonge, L. Ulloa, Br. J. Pharmacol. 151 (2007) 915–929;
M. Rosas-Ballina, K.J. Tracey, J. Intern. Med. 265 (2009) 663–679;
c) M.S. Gurun, R. Parker, J.C. Eisenach, M. Vincler, Anesth. Analg. 108 (2009) 1680–1687;
d) J.-M. Waldburger, G.S. Firestein, Curr. Rheumatol. Rep. 12 (2010) 370–378.
[9] A. Pacini, L. Di Cesare Mannelli, L. Bonaccini, S. Ronzoni, A. Bartolini, C. Ghelardini, Pain 150 (2010) 542–549.
[10] W.H. Bunnelle, K.R. Tietje, J.M. Frost, D. Peters, J. Ji, T. Li, M.J.C. Scanio, L. Shi, D.J. Anderson, T. Dyhring, J.H. Grønlien, H. Ween, K. Thorin-Hagene, M.D. Meyer, J. Med. Chem. 52 (2009) 4126–4141.
[11] a) L. Rizzi, C. Dallanoce, C. Matera, P. Magrone, L. Pucci, C. Gotti, F. Clementi, M. De Amici, Bioorg. Med. Chem. Lett. 18 (2008) 4651–4654;
b) G. Grazioso, D.Y. Pomè, C. Matera, F. Frigerio, L. Pucci, C. Gotti, C. Dallanoce, M. De Amici, Bioorg. Med. Chem. Lett. 19 (2009) 6353–6357;
c) C. Dallanoce, P. Magrone, C. Matera, L. Lo Presti, M. De Amici, L. Riganti, F. Clementi, C. Gotti, C. De Micheli, Eur. J. Med. Chem. 45 (2010) 5594–5601.
[12] a) C. De Micheli, M. De Amici, C. Dallanoce, F. Clementi, C. Gotti, PCT Int. Appl. (2008) 47 WO 2008000469;
b) C. Dallanoce, P. Magrone, C. Matera, F. Frigerio, G. Grazioso, M. De Amici, S. Fucile, V. Piccari, K. Frydenvang, L. Pucci, C. Gotti, F. Clementi, C. De Micheli, Chem. Med. Chem. 6 (2011) 889–903.
[13] a) S.M. Jenkins, H.J. Wadsworth, S. Bromidge, D.S. Orlek, P.A. Wyman, G.J. Riley, J. Hawkins, J. Med. Chem. 35 (1992) 2392–2406;
b) P.H. Olesen, P. Sauerberg, T.G. Petersen, S. Treppendhal, B. Bentzen, J. Deeter, J.S. Ward, C.H. Mitch, S.V. Lehmann, Chirality 9 (1997) 739–749.
[14] a) D.M. Vyas, Y. Chiang, T.W. Doyle, Tetrahedron Lett. 25 (1984) 487–490;
b) G.A. Lee, Synthesis 6 (1982) 508–509;
[15] P.J. Munson, D. Rodbard, Anal. Biochem. 107 (1980) 220–239.
[16] a) N. Zaveri, F. Jiang, C. Olsen, W. Polgar, L. Toll, J. Med. Chem. 53 (2010) 8187–8191;
b) K. Poth, T.J. Nutter, J. Cuevas, M.J. Parker, D.J. Adams, C.W. Luetje, J. Neurosci. 17 (1997) 586–596.
[17] a) G. Mullen, J. Napier, M. Balestra, T. DeCory, G. Hale, J. Macor, R. Mack, J. Loch 3rd, E. Wu, A. Kover, P. Verhoest, A. Sampognaro, E. Phillips, Y. Zhu, R. Murray, R. Griffith, J. Blosser, D. Gurley, A. Machulskis, J. Zongrone, A. Rosen, J. Gordon, J. Med. Chem. 43 (2000) 4045–4050;
b) F.M. Leonik, R.L. Papke, N.A. Horenstein, Bioorg. Med. Chem. Lett. 17 (2007) 1520–1522.
[18] G. Grazioso, A. Cavalli, M. De Amici, M. Recanatini, C. De Micheli, J. Comp. Chem. 29 (2008) 2593–2602.
[19] V. Gerzanich, X. Peng, F. Wang, G. Wells, R. Anand, S. Fletcher, J. Lindstrom, Mol. Pharmacol. 48 (1995) 774–782.
[20] Y.C. Cheng, W.H. Prusoff, Biochem. Pharmacol. 22 (1973) 3099–3108.
[21] S. Fucile, M. Renzi, P. Lax, F. Eusebi, Cell Calcium 34 (2003) 205–209.
[22] M.J. Frisch, G.W. Trucks, H.B. Schlegel, G.E. Scuseria, M.A. Robb, J.R. Cheeseman, G. Scalmani, V. Barone, B. Mennucci, G.A. Petersson, H. Nakatsuji, M. Caricato, X. Li, H.P. Hratchian, A.F. Izmaylov, J. Bloino, G. Zheng, J.L. Sonnenberg, M. Hada, M. Ehara, K. Toyota, R. Fukuda, J. Hasegawa, M. Ishida, T. Nakajima, Y. Honda, O. Kitao, H. Nakai, T. Vreven, J.A. Montgomery Jr., J.E. Peralta, F. Ogliaro, M. Bearpark, J.J. Heyd, E. Brothers, K.N. Kudin, V.N. Staroverov, R. Kobayashi, J. Normand, K. Raghavachari, A. Rendell, J.C. Burant, S.S. Iyengar, J. Tomasi, M. Cossi, N. Rega, J.M. Millam, M. Klene, J.E. Knox, J.B. Cross, V. Bakken, C. Adamo, J. Jaramillo, R. Gomperts, R.E. Stratmann, O. Yazyev, A.J. Austin, R. Cammi, C. Pomelli, J.W. Ochterski, R.L. Martin, K. Morokuma, V.G. Zakrzewski, G.A. Voth, P. Salvador, J.J. Dannenberg, S. Dapprich, A.D. Daniels, Ö Farkas, J.B. Foresman, J.V. Ortiz, J. Cioslowski, D.J. Fox, Gaussian 09, Revision A.02. Gaussian, Inc., Wallingford CT, 2009.
[23] The PyMOL Molecular Graphics System, Version 0.99, Schrödinger, LLC.
[24] GOLD v. 4.0, Cambridge Crystallographic data Centre: Cambridge, UK.
[25] Tripos Inc., 1699 South Hanley Rd., St. Louis, MO 63144.